



# Non-dimensional size effects on the thermodynamic properties of solids

R.S. Prasher, P.E. Phelan\*

Arizona State University, Department of Mechanical and Aerospace Engineering, Tempe, AZ 85287-6106, U.S.A.

Received 7 April 1998; in final form 25 August 1998

---

## Abstract

Although a number of analyses have been presented on the size effects on transport properties like the thermal conductivity, very few studies have focused on size effects on thermodynamic properties like the heat capacity. The present analysis considers the effect of size on thermodynamic properties when the dimension in one, two or all three directions is extremely small, leading to a reduction in the number of phonon wave vectors. The results are presented in a novel non-dimensional form, so that the effect of dimension on the thermal properties of any material can be easily obtained once the bulk properties are known. © 1998 Elsevier Science Ltd. All rights reserved.

---

## Nomenclature

$A$  constant in equation (25)  
 $a$  lattice constant [ $\text{\AA}$ ]  
 $C$  heat capacity [J]  
 $c$  heat capacity per unit volume [ $\text{J m}^{-3}$ ]  
 $f$  Helmholtz energy per unit volume [ $\text{J m}^{-3}$ ]  
 $F$  intermediate function for calculating heat capacity  
 $g$  Gibbs energy per unit volume [ $\text{J m}^{-3}$ ]  
 $h$  enthalpy per unit volume [ $\text{J m}^{-3}$ ]  
 $\hbar$  Planck's constant divided by  $2\pi = 1.054496 \times 10^{-34}$  J s  
 $H$  represents any thermodynamic property  
 $k$  wave vector [ $\text{m}^{-1}$ ]  
 $k_b$  Boltzmann constant =  $1.38062 \times 10^{-23}$  J K $^{-1}$   
 $k_d$  Debye wave vector [ $\text{m}^{-1}$ ]  
 $K$  spring constant [ $\text{kg s}^{-2}$ ]  
 $L$  length [ $\text{\AA}$ ]  
 $m$  mass of an atom [kg]  
 $m_{\max}$  maximum index of summation  
 $n$  atomic density [ $\text{m}^{-3}$ ]  
 $N$  number of atoms or number of atomic layers  
 $r$  distance between two atoms [ $\text{\AA}$ ]  
 $r_0$  nearest neighbor separation at equilibrium [ $\text{\AA}$ ]  
 $R$  non-dimensional parameter

$s$  entropy per unit volume [ $\text{J m}^{-3} \text{K}^{-1}$ ]  
 $T$  temperature [K]  
 $u$  internal energy per unit volume [ $\text{J m}^{-3}$ ].

## Greek symbols

$\alpha$  quantum fluctuation parameter  
 $\beta$  effective temperature  
 $\Delta k$  small element of the wave vector [ $\text{m}^{-1}$ ]  
 $\Delta p$  uncertainty in the momentum [ $\text{kg m s}^{-1}$ ]  
 $\Delta x$  uncertainty in the position [m]  
 $\varepsilon$  ratio of the exact number of points within  $k$  space to the number of points for a  $k$  space of spherical shape  
 $\theta$  Debye temperature [K]  
 $\lambda_c$  critical phonon wavelength [m]  
 $\Lambda$  mean free path of phonons [m]  
 $v$  speed of sound [ $\text{m s}^{-1}$ ]  
 $\xi$  parameter in Lennard–Jones potential [J]  
 $\Pi$  number of atoms per unit cell  
 $\sigma$  parameter in Lennard–Jones potential [m]  
 $\phi$  Lennard–Jones potential [J]  
 $\Psi$  function representing size effects on various thermodynamic parameters  
 $\omega$  phonon angular frequency [ $\text{rad s}^{-1}$ ].

## Subscripts

exact exact number of points in  $k$  space  
 $i, j$  indices  
int integration

---

\* Corresponding author. Tel.: 001 602 965 1625; fax: 001 602 965 1384; e-mail: phelan@asu.edu

spherical  $k$  space of spherical shape  
 sum summation  
 $x, y, z$  directional coordinates.

## 1. Introduction

Thin films play a major role in modern-day electronics, where the size effects are due to a reduction in only one dimension, i.e., in the film thickness direction. A wide range of micro- and nanoscale devices that do not fall into the category of thin films, meaning that size effects are due to reduced dimensions along two or three directions, are also important in this era of microscale device technology. Some of these devices are quantum wires [1] and quantum dots [2].

Pronounced size effects on the thermal conductivity of such micro structures have received considerable attention over the past decade, with the results summarized in two recent review articles [3, 4]. Although thermodynamic properties are known to exhibit size effects, very little has been done in the past to consider such effects in a practically useful manner for engineering calculations. Recent investigation by the authors, however, demonstrated a pronounced size effect on the thermodynamic properties of thin films due to the absence of a large number of wave vectors ( $k$ ) or equivalently, states, in a thin-film structure [5, 6]. Some of the other prominent calculations on the heat capacity are by Grille et al. [7] and McGurn et al. [8]. Prasher and Phelan [5, 6] used the Debye model and the results were presented in a new non-dimensional form, which accurately described the thermal properties of thin films. Prasher and Phelan [5, 6] also demonstrated that the Debye temperature remains constant as opposed to that suggested by Grille et al. [7]. The effect of such stratified  $k$  values is expected to be more pronounced for structures with reduced dimensions along two or all three mutually perpendicular directions. Consequently, the present analysis examines size effects on the thermodynamic properties due to reductions in the dimensions along two or three directions.

At these minute scales it is also expected that the Debye model will not hold even at low temperatures, whereas for the bulk material it works well at low temperatures. The phonon dispersion is thus calculated using the Born–von Kármán model and the Debye model. Any structure that shows size effects due to a reduced dimension along one direction is referred to as a 1-D (one-dimensional) structure, e.g. a thin film, along two directions 2-D and along all three directions as 3-D. Analogous to the previous non-dimensionalization of results for a 1-D structure [5, 6], a non-dimensionalization for 2- and 3-D structures is also suggested, which nicely describes the size effects in a universal manner. The analysis is further carried out for other thermodynamic properties such as entropy. The results are also compared with the cal-

ulation of McGurn et al. [8] for the size effects on the heat capacity of a linear chain of atoms.

## 2. Size effect on the phonon heat capacity

A simple lattice is considered as shown in Fig. 1. It is assumed that the lattice is simple cubic with the generalization that the number of atoms per unit volume, or the atomic density ( $n$ ), is that of the actual lattice structure. If the numbers of atoms in the  $x$ -,  $y$ - and  $z$ -directions are  $N_x + 1$ ,  $N_y + 1$  and  $N_z + 1$ , respectively, then

$$N_x = \frac{L_x}{a}, \quad N_y = \frac{L_y}{a}, \quad N_z = \frac{L_z}{a} \quad (1)$$

where  $L_x$ ,  $L_y$  and  $L_z$  are the lengths of the 3-D lattice in the  $x$ -,  $y$ - and  $z$ -directions, respectively and  $a$  is the lattice constant. The set of allowed wave vectors  $k$ , assuming periodic boundary conditions, is given by [9]:

$$\begin{aligned} k_x &= 0; \quad \pm \frac{2\pi}{L_x}; \quad \pm \frac{4\pi}{L_x} \dots \frac{N_x\pi}{L_x}, \quad \Delta k_x = \frac{2\pi}{L_x} = \frac{2\pi}{N_x a} \\ k_y &= 0; \quad \pm \frac{2\pi}{L_y}; \quad \pm \frac{4\pi}{L_y} \dots \frac{N_y\pi}{L_y}, \quad \Delta k_y = \frac{2\pi}{L_y} = \frac{2\pi}{N_y a} \\ k_z &= 0; \quad \pm \frac{2\pi}{L_z}; \quad \pm \frac{4\pi}{L_z} \dots \frac{N_z\pi}{L_z}, \quad \Delta k_z = \frac{2\pi}{L_z} = \frac{2\pi}{N_z a} \end{aligned} \quad (2)$$

where  $k_x$ ,  $k_y$  and  $k_z$  are the components of  $k$  in the  $x$ -,  $y$ - and  $z$ -directions, respectively and satisfy

$$k^2 = k_x^2 + k_y^2 + k_z^2 \quad (3)$$

and  $\Delta k_x$ ,  $\Delta k_y$  and  $\Delta k_z$  are the differences in consecutive discrete  $k$  along the corresponding directions.

In the traditional approach, i.e., when the number of atoms in all directions is large, then the number of allowed states per unit volume in a  $k$  space of spherical shape is simply  $n$ , given by

$$n = \frac{N}{V} = \frac{1}{(2\pi)^3} \iiint dk_x dk_y dk_z = \frac{1}{(2\pi)^3} \left( \frac{4\pi k^3}{3} \right) \quad (4)$$

where the limits taken by  $k_x$ ,  $k_y$  and  $k_z$  are

$$\begin{aligned} -\sqrt{k_d^2 - k_x^2 - k_y^2} &\leq k_z \leq \sqrt{k_d^2 - k_x^2 - k_y^2}, \\ -\sqrt{k_d^2 - k_x^2} &\leq k_y \leq \sqrt{k_d^2 - k_x^2}, \\ \text{and } -k_d &\leq k_x \leq k_d \end{aligned} \quad (5)$$

and where the Debye vector,  $k_d$ , is calculated from [9]

$$k_d = (6\pi^2 n)^{1/3}. \quad (6)$$

Now if the number of atoms along any direction is very small, then the number of states calculated by equation (4) is not exactly valid, as the volume of the cuboid of sides  $2\pi/L_x$ ,  $2\pi/L_y$  and  $2\pi/L_z$  is large compared to the surface bounded by the  $k$  space, which will no longer be spherical in shape. A quantity  $\varepsilon$  is defined as the ratio of the exact number of points in  $k$  space ( $N_{\text{exact}}$ ) to the number of points given by equation (4) ( $N_{\text{spherical}}$ ) [5, 6]:

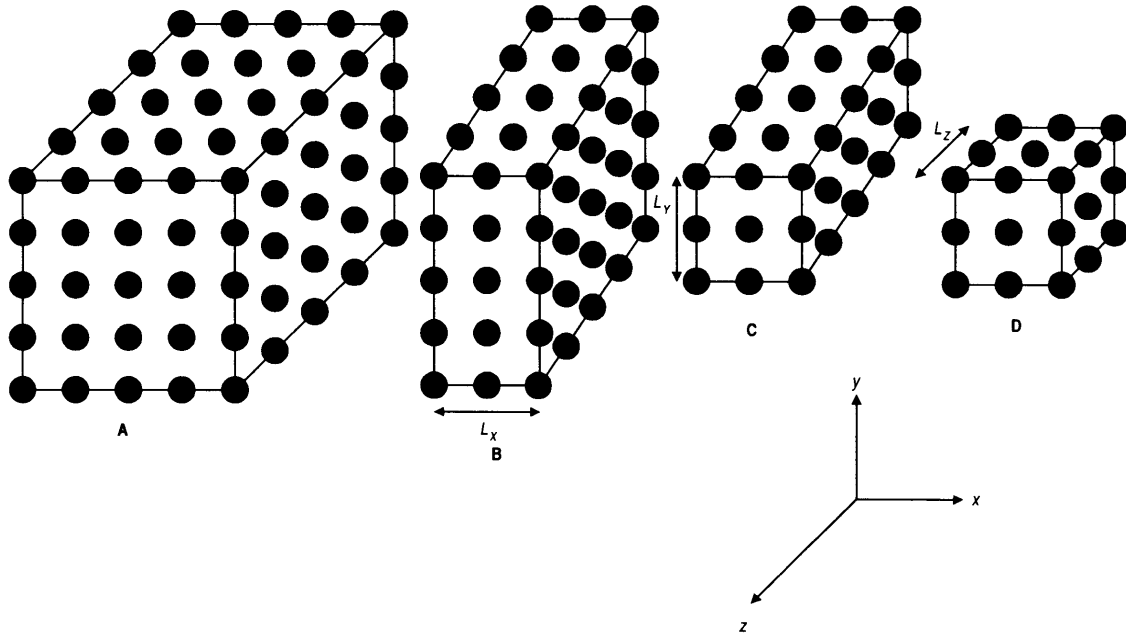


Fig. 1. (A) A bulk lattice structure. (B) A 1-D structure. (C) A 2-D structure. (D) A 3-D structure.

$$\epsilon = \frac{N_{\text{exact}}}{N_{\text{spherical}}} \tag{7}$$

To simplify the analysis, this ratio is calculated only for  $k = \pi/a$ , the Brillouin zone wave vector. For  $N_{\text{exact}}$ , from equation (2)  $k_x$  and  $k_y$  for the first quadrant are given by:

$$k_{x_i} = \Delta k_x i = \left(\frac{2\pi}{N_x a}\right) i, \quad i = 0 \dots \frac{N_x}{2}$$

and

$$k_{y_j} = \Delta k_y j = \left(\frac{2\pi}{N_y a}\right) j, \quad j = 0 \dots m_y \tag{8}$$

where the value taken by  $m_y$  is specified as shown below. From equation (3) we have

$$k_y^2 + k_z^2 = \frac{\pi^2}{a^2} - k_{x_i}^2 \tag{9}$$

which is the equation of a circle of radius  $(\pi^2/a^2 - k_{x_i}^2)^{1/2}$ . Therefore,  $m_y$  is

$$m_y = \frac{\text{maximum value of } k_{y_j}}{2\pi/N_y a} = \frac{\sqrt{\frac{\pi^2}{a^2} - k_{x_i}^2}}{2\pi/N_y a} = \frac{N_y}{2} \sqrt{1 - \frac{4i^2}{N_x^2}} \tag{10}$$

which is rounded to the nearest integer.

The number of points lying along the line joining the points  $k_z = 0$  and  $k_z = k_{z_{i,j}}$  becomes

$$N_{z_{i,j}} = \frac{k_{z_{i,j}}}{2\pi/L_z} = \frac{N_z}{2} \sqrt{1 - \frac{4i^2}{N_x^2} - \frac{4j^2}{N_y^2}} \tag{11}$$

The total number of points in the  $k$  space is obtained by summing up all the points at each  $k_{x_i}$  and  $k_{y_j}$  in the first quadrant and multiplying by eight:

$$N_{\text{exact}} = 4N_z \sum_0^{N_x/2} \sum_0^{m_y} \sqrt{1 - \frac{4i^2}{N_x^2} - \frac{4j^2}{N_y^2}} \tag{12}$$

From its definition in equation (7),  $\epsilon$  is expressed as:

$$\epsilon = \frac{24 \sum_0^{N_x/2} \sum_0^{m_y} \sqrt{1 - \frac{4i^2}{N_x^2} - \frac{4j^2}{N_y^2}}}{\pi N_x N_y} \tag{13}$$

Strictly speaking this only gives a very conservative estimate of  $\epsilon$ . Although  $\epsilon$  has been treated as a constant, in general  $\epsilon$  is a function of  $k$  [5].

In order to evaluate the heat capacity at constant volume ( $C$ ), equation (4) is rewritten by incorporating  $\epsilon$ :

$$n = \frac{N}{V} = \frac{1}{(2\pi)^3} \iiint \epsilon dk_x dk_y dk_z = \frac{\epsilon}{(2\pi)^3} \iiint dk_x dk_y dk_z \tag{14}$$

Since the values taken by  $k_x$  and  $k_y$  are discrete on the scale of  $2\pi/L_x$  and  $2\pi/L_y$ , the triple integral in equation (14) cannot be carried out, leading to its replacement by summation. Evaluation of the above integral by sum-

mation will lead to the appropriate calculation of  $k_d$ . However,  $k_d$  given by using summation does not differ much from the classical value [equation (6)] because of the opposing effects of  $\varepsilon$  and the replacement of the integral in equation (14) by summation [5]. If  $\varepsilon$  is not taken into consideration then  $k_d$  will increase compared to the bulk case [5, 6], thereby increasing the Debye temperature as suggested by Grille et al. [7]. Here, for simplicity the value of  $k_d$  is given by equation (6).

The calculation of  $C$  by incorporating the above analysis is achieved as follows.

Regardless of the model,  $C$  can be expressed as [10]

$$C = 3 \frac{\partial}{\partial T} \sum_T \frac{\hbar \omega}{\exp\left(\frac{\hbar \omega}{k_b T}\right) - 1} \quad (15)$$

where  $\hbar$  is Planck's constant divided by  $2\pi$ ,  $k_b$  the Boltzmann constant,  $T$  the temperature and  $\omega$  the phonon angular frequency.

### 2.1. Debye model

In the traditional approach for relatively large samples equation (15) can be replaced by an integral:

$$c_{\text{sum}} = 24 \frac{\varepsilon \hbar v}{(2\pi)^3} \frac{\partial}{\partial T} \sum_{k_x, k_y} \left[ \int_0^{\sqrt{k_d^2 - k_x^2 - k_y^2}} \frac{\sqrt{k_x^2 + k_y^2 + k_z^2}}{\exp\left(\frac{\hbar v \sqrt{k_x^2 + k_y^2 + k_z^2}}{k_b T}\right) - 1} dk_z \right] \Delta k_x \Delta k_y \quad (20)$$

The above summation can be simplified as:

$$c_{\text{sum}} = 24 \frac{\varepsilon \hbar^2 v^2}{(2\pi)^3 k_b T^2} \sum_{i=1}^{m_{\text{max}_x}} \sum_{j=1}^{m_{\text{max}_y}} F(k_{x_i}, k_{y_j}) \Delta k_x \Delta k_y \quad (21)$$

and where

$$F(k_{x_i}, k_{y_j}) = \int_0^{\sqrt{k_d^2 - (i\Delta k_x)^2 - (j\Delta k_y)^2}} \frac{[(i\Delta k_x)^2 + (j\Delta k_y)^2 + k_z^2] \exp\left(\frac{\hbar v \sqrt{(i\Delta k_x)^2 + (j\Delta k_y)^2 + k_z^2}}{k_b T}\right)}{\left[\exp\left(\frac{\hbar v \sqrt{(i\Delta k_x)^2 + (j\Delta k_y)^2 + k_z^2}}{k_b T}\right) - 1\right]^2} dk_z \quad (22)$$

$$c = c_{\text{int}} = \frac{3}{(2\pi)^3} \frac{\partial}{\partial T} \iiint \frac{\hbar \omega}{\exp\left(\frac{\hbar \omega}{k_b T}\right) - 1} dk_x dk_y dk_z \quad (16)$$

where  $c_{\text{int}}$  is the heat capacity per unit volume calculated by integration. Using the Debye approximation,  $\omega = vk$ , where  $v$  is the speed of long wavelength sound waves, the above equation can be reduced to

$$c_{\text{int}} = 9nk_b \left(\frac{T}{\theta}\right)^3 \int_0^{\theta/T} \frac{X^4 \exp(X)}{[\exp(X) - 1]^2} dX \quad (17)$$

where  $\theta$  is the Debye temperature.

When the number of atoms along any direction is very small, then the replacement of the summation in equation (15) by an integral is not valid along the direction of fewer atoms. The Debye model reduces equation (15) to

$$C = 3 \frac{\partial}{\partial T} \sum_k \frac{\hbar v k}{\exp\left(\frac{\hbar v k}{k_b T}\right) - 1} \quad (18)$$

The heat capacity per unit volume calculated by summation ( $c_{\text{sum}}$ ) can be written as [5]

$$c_{\text{sum}} = 3 \frac{\varepsilon \hbar v}{(2\pi)^3} \frac{\partial}{\partial T} \times \sum_{k_x} \sum_{k_y} \sum_{k_z} \frac{\sqrt{k_x^2 + k_y^2 + k_z^2}}{\exp\left(\frac{\hbar v \sqrt{k_x^2 + k_y^2 + k_z^2}}{k_b T}\right) - 1} \Delta k_x \Delta k_y \Delta k_z \quad (19)$$

The limits of  $k_x$ ,  $k_y$ , and  $k_z$  are given by equation (5). For now, consider that we are investigating the size effects only along the  $x$ - and  $y$ -directions (Fig. 1c) (i.e., a 2-D structure) and thus the summation over  $z$  can still be replaced by an integral, leading to

where

$$k_x = i\Delta k_x, \quad i = 1 \dots m_{\text{max}_x}$$

$$k_y = j\Delta k_y, \quad j = 1 \dots m_{\text{max}_y}$$

$$m_{\text{max}_x} = \left(\frac{k_d}{2\pi}\right) N_x a \quad (\text{rounded to the nearest integer})$$

$$m_{\text{max}_y} = \left(\frac{\sqrt{k_d^2 - (i\Delta k_x)^2}}{2\pi}\right) N_y a$$

(rounded to the nearest integer).

2.2. Born–von Kàrmàn model for dispersion

The use of the Debye model is questionable for the structures mentioned in this paper because of the discreteness of  $k$  along the direction of fewer atoms, even at very low temperatures, where it is expected to be applicable for the bulk case. To observe the effect of dispersion, the Born–von Kàrmàn model is applied and the results are compared with the Debye model in Fig. 2, which is discussed later.

The dispersion relation is given as [11]

$$\omega = \frac{2vk_d}{\pi} \times \sqrt{\left\{ \sin^2 \left( \frac{k_x \pi}{2k_d} \right) + \sin^2 \left( \frac{k_y \pi}{2k_d} \right) + \sin^2 \left( \frac{k_z \pi}{2k_d} \right) \right\}} \quad (23)$$

which can be easily reduced to the Debye model for very small values of  $k$ , i.e., when the number of atoms is very high. Thus  $c_{int}$  is now determined by replacing  $\omega$  with equation (23) in equation (16).

Similarly  $c_{sum}$  can be obtained by substituting  $\omega$  from equation (23) in equation (15) and carrying out the summation of  $k_x$  and  $k_y$ , and the integration over  $k_z$ , as was done for the Debye model.

3. Results

The calculation of the heat capacity utilizing the above analysis is performed for different materials of primary importance to the semiconductor industry. The physical data for the materials of consideration are given in [5]. Figure 2 presents the results of the Debye and the dispersion (Born–von Kàrmàn) models, in which the ratio of  $c$  calculated by summation and integration is plotted vs.  $N_x$ , with  $N_y$  and  $T$  other variable parameters. The ratio  $c_{sum}/c_{int}$  is practically the same for both models. This revelation is not at all surprising, because the size effects are prominent only in the region where  $c$  is proportional to  $T^3$  [5, 6]. Although  $k$  is quite large for the microscale case, the excited  $k$  at low temperatures are still small enough to reduce the Born–von Kàrmàn model to the Debye model. The Born–von Kàrmàn model differs from the Debye model in the intermediate temperature range, where the effect of thickness on the thermodynamic properties ceases to exist. The decrease in the heat capacity of these microstructures is due to the large magnitude of  $k$ , resulting in a reduction in the number of excited phonons. Figure 2 also shows that increasing  $N_y$ , increasing  $N_x$  and increasing  $T$  increases  $c_{sum}/c_{int}$ . Keeping this in mind, analogous to the analysis of [5, 6], a non-

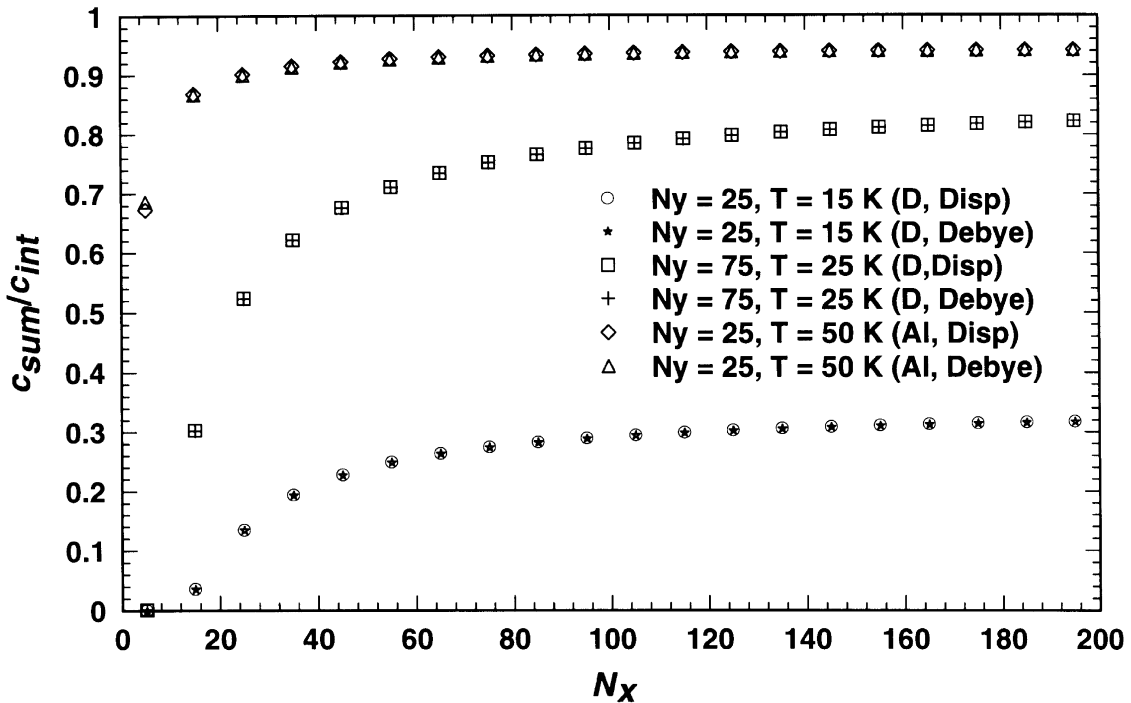


Fig. 2. Heat capacity ratio for 2-D structures calculated using the Debye and the dispersion ('disp') relations, vs. the number of atomic layers in the  $x$ -direction, where 'D' and 'Al' refer to diamond and aluminum, respectively.

dimensionalization of the results is achieved by applying the following argument.

It can be shown [5, 6] for the 2-D case that, based on the Debye model,

$$\frac{c_{\text{sum}}}{c_{\text{int}}} = \left(1 + \frac{h\nu k}{2k_b T}\right)^{-3} = 1 - 3\frac{h\nu k}{2k_b T} + \dots \quad (24)$$

The wave vector  $k$  in equation (24) can be conveniently replaced by  $k = \sqrt{(\Delta k_x)^2 + (\Delta k_y)^2}$  because the maximum contribution to the excited modes will come from the  $k$  given by this value. Therefore,

$$\begin{aligned} \frac{c_{\text{sum}}}{c_{\text{int}}} &= 1 - 3\frac{h\nu\sqrt{(\Delta k_x)^2 + (\Delta k_y)^2}}{2k_b T} \\ &= 1 - \frac{A\theta}{T} \sqrt{\frac{1}{N_x^2} + \frac{1}{N_y^2}} = 1 - \frac{A\theta}{TN_{\text{eff}}} \quad (25) \end{aligned}$$

where  $A$  is a constant and

$$N_{\text{eff}} = \frac{1}{\sqrt{1/N_x^2 + 1/N_y^2}} = \frac{N_x N_y}{\sqrt{N_x^2 + N_y^2}} \quad (26)$$

Similarly for the 3-D case it can be shown that

$$\begin{aligned} N_{\text{eff}} &= \frac{1}{\sqrt{1/N_x^2 + 1/N_y^2 + 1/N_z^2}} \\ &= \frac{N_x N_y N_z}{\sqrt{(N_x N_y)^2 + (N_y N_z)^2 + (N_z N_x)^2}} \quad (27) \end{aligned}$$

Equation (25) suggests that non-dimensionalization of the results can be easily achieved by plotting  $c_{\text{sum}}/c_{\text{int}}$  vs. the parameter  $N_{\text{eff}}T/\theta$ , where  $N_{\text{eff}}$  is given by equation (26) for 2-D structures and equation (27) for 3-D structures. The results of the 2-D case for a variety of materials having either a diamond or a FCC lattice structure are given in Fig. 3. It is to be noted that if either  $N_x$ ,  $N_y$ , or both are large, then  $N_{\text{eff}}$  given by equation (27) reduces to the  $N_{\text{eff}}$  of 2- and 1-D structures, respectively. Therefore,  $N_{\text{eff}}$  given by equation (27) is a general form of  $N_{\text{eff}}$ , which describes 1-, 2- and 3-D structures simultaneously.

A similar non-dimensionalization is performed for 3-D structures, by replacing the integration over  $k_z$  by a summation in equation (20). The results for the 3-D case are shown in Fig. 4. Along with the 3-D case, analytical fits for the 1-D [5, 6] and 2-D cases are also plotted for comparison. It is seen from Figs 3 and 4 that all the points for different combinations of  $N_x$ ,  $N_y$ ,  $N_z$  and  $\theta$  do not fall exactly on the same curve, whereas for the 1-D case all these points fall very elegantly on the same curve [5, 6]. One of the reasons for this is approximating the upper limit of the summations in equation (21) to its nearest integer. The error caused by this increases as the dimensionality of the system increases because of the increasing number of summations.

The values of the coefficients in equation (25) and expanded to an additional term for 2- and 3-D structures, found by fitting to the calculated results are presented in

Table 1. The form of the fit for the 2- and 3-D cases is determined by carrying out the expansion in equation (24) to a higher order, since the magnitude of  $k$  is larger for the 2- and 3-D cases compared to the magnitude of  $k$  for the 1-D case. The results of Table 1 also indicate that the signs of the fitted coefficients match with the signs of the coefficients given by equation (24). The analytical solution presented in Table 1 gives the expression till the second-order for both the 2- and 3-D structures, as the higher order terms are negligibly small. Utilizing the expressions in Table 1 allows the calculation of the heat capacity for any microstructure, provided the bulk value ( $c_{\text{int}}$ ) is known. A sample calculation for a 3-D silicon structure of 100 Å in all directions, at a temperature 50 K, gives a 22% reduction in  $c$  from its bulk value.

The size effect on heat capacity described in this paper and the earlier work on thin films by the same authors [5, 6] is compared with the analysis by McGurn et al. [8]. McGurn et al. [8] computed the size effects on the heat capacity of a linear chain of atoms by applying Monte Carlo simulation for the anharmonic interaction and lattice dynamics for the harmonic interaction. They used the Lennard–Jones potential function in their calculation. The Lennard–Jones potential,  $\phi(r)$ , is given by [9]

$$\phi(r) = \xi \left[ \left(\frac{\sigma}{r}\right)^{12} - \left(\frac{\sigma}{r}\right)^6 \right] \quad (28)$$

where  $\xi$  and  $\sigma$  are the parameters in the Lennard–Jones potential and  $r$  is the nearest neighbor separation. In the harmonic approximation, the frequency of oscillation of the atoms,  $\omega$ , is given by [9]

$$\omega = 2\sqrt{\frac{K}{m}} \sin\left(\frac{ka}{2}\right) \quad (29)$$

where  $K$ , the spring constant for the harmonic approximation, is given by

$$K = \left[ \frac{d^2\phi(r)}{dr^2} \right]_{r=r_0} \quad (30)$$

and where  $r_0 = 2^{1/6}\sigma$  is the equilibrium nearest neighbor separation. Equations (28) and (30) yield  $K$  as:

$$K = 57.145\xi\sigma^{-2}. \quad (31)$$

Under the Debye assumption  $\omega$  can be simplified as

$$\omega = \left(\sqrt{\frac{K}{m}}a\right)k = vk \quad (32)$$

and therefore,

$$v = \sqrt{\frac{K}{m}}a = \sqrt{\frac{57.145\xi}{m}}\frac{a}{\sigma}. \quad (33)$$

The Debye temperature  $\theta$  for the system is given by [9]

$$\theta = \frac{h\nu k_d}{k_b} = \frac{7.56h}{k_b} \sqrt{\frac{\xi}{m}} \frac{a}{\sigma} k_d \quad (34)$$

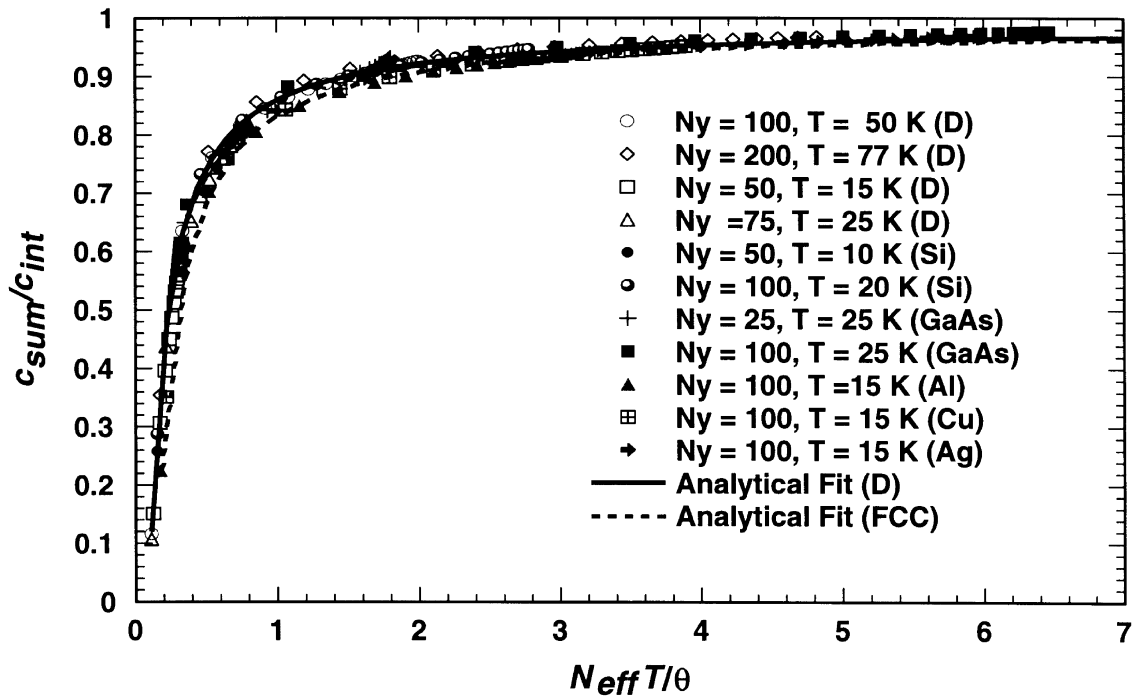


Fig. 3. Heat capacity ratio for 2-D structures vs. the non-dimensional parameter  $N_{eff}T/\theta$ .

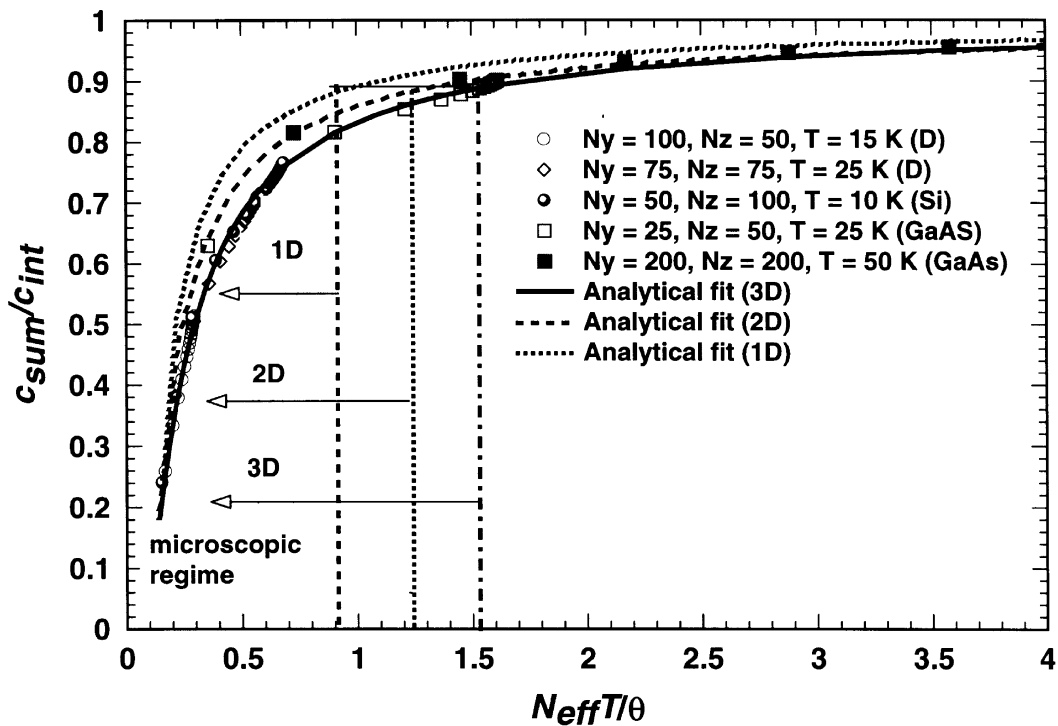


Fig. 4. Comparison of the size effects for 1-, 2- and 3-D structures.

Table 1  
Values of  $N_{\text{eff}}$  and the analytical curve fits for 1-, 2- and 3-D geometries, where  $R = N_{\text{eff}}T/\theta$

Case	$N^{\text{eff}}$	$c_{\text{sum}}/c_{\text{int}}$ (diamond lattice)	$c_{\text{sum}}/c_{\text{int}}$ (FCC lattice)
1-D	$N_x$	$0.9932 - 0.102/R$	$0.985 - 0.1177/R$
2-D	$\frac{N_x N_y}{\sqrt{N_x^2 + N_y^2}}$	$0.985 - 0.1292/R + 0.00357/R^2$	$0.9856 - 0.1575/R + 0.0043/R^2$
3-D	$\frac{N_x N_y N_z}{\sqrt{(N_x N_y)^2 + (N_y N_z)^2 + (N_z N_x)^2}}$	$0.9987 - 0.1755/R + 0.00847/R^2$	$0.9855 - 0.1668/R + 0.0087/R^2$

where  $k_d = \pi/a$  (same as the Brillouin Zone) for a 1-D system.  $\theta$  can be further simplified as

$$\theta = 23.75 \frac{\alpha \zeta}{k_b} \quad (35)$$

where  $\alpha = \hbar/\sqrt{m\xi}\sigma$  is a measure of quantum fluctuation as described by McGurn et al. [8]. The heat capacity of a linear chain at very low temperatures is given by [9]

$$\frac{C}{Nk_b} = 3 \left( \frac{T}{\theta} \right) = \frac{0.1263}{\alpha \zeta \beta} \quad (36)$$

where  $\beta = 1/k_b T$ .

McGurn et al. [8] gives  $C$  as

$$\frac{C}{Nk_b} = \left[ \frac{0.1385}{\alpha \zeta \beta} - \frac{0.376}{\xi \beta} \right] \quad (37)$$

where the second term on the right-hand-side of equation (37) represents the anharmonic contribution. Thus under the harmonic approximation the second term is eliminated, leaving

$$\frac{C}{Nk_b} = \frac{0.1385}{\alpha \zeta \beta}. \quad (38)$$

Comparing equations (36) and (38), it is seen that the numerators of both equations are almost the same. In order to maintain the uniformity of the calculations, the value suggested by McGurn et al. [8] (0.1385) is used for both equations, yielding

$$\frac{T}{\theta} = \frac{0.04616}{\alpha \zeta \beta}. \quad (39)$$

In order to compare with our results, we need to express those of McGurn et al. [8] in the form of the same ratio,  $c_{\text{sum}}/c_{\text{int}}$ , or in other words, the microscale  $c$  divided by the bulk  $c$ . Although McGurn et al. [8] report that  $N = 15$  represents an infinite linear chain,  $N = 15$  does not represent an infinite chain for  $\beta \zeta = 10$  and  $\alpha = 0.1$ ,

because the value of  $c$  calculated by lattice dynamics theory for this configuration is much less than that given by equation (38). This is not surprising as this configuration represents a system at very low temperature, or a material of high  $\theta$ . Therefore, for this configuration  $c$  is taken to be the microscale  $c$  and is non-dimensionalized by the bulk value of  $c$  given by equation (38). For their other configurations at different values of  $\alpha$ ,  $\zeta$  and  $\beta$ ,  $c_{\text{sum}}/c_{\text{int}}$  is determined by dividing  $c$  for  $N = 10$  for different values of  $\alpha$ ,  $\zeta$  and  $\beta$  by the corresponding  $c$  for  $N = 15$ .

We assume that the size effects on a 1-D chain are equivalent to the size effects on the 3-D structure shown in Fig. 1, because although a 3-D structure has three directions associated with it, it has size effects in all the three directions, i.e., 100% of the directions are size affected. Similarly, a finite 1-D chain has only one direction associated with it and therefore, 100% of its directions are size affected. Since the ratio of  $c_{\text{sum}}$  and  $c_{\text{int}}$  is being compared, not the absolute magnitude, the 3-D structure and the 1-D chain should give the same results. Thus, for comparison, the equation for a 3-D structure given in Table 1 will be used, specifically the equation for the diamond-type lattice.

Figure 5 shows that the trends of the present results and those of McGurn et al. [8] agree. Although there are some apparent differences, the onset of the microscopic regime is the same from both calculations. There is a greater deviation in the results of McGurn et al. [8] and the present analysis at low temperatures. Some of the possible reasons for this deviation are: (i) the replacement of the numerator in equation (36) (0.1263) by the value suggested by McGurn et al. [8] (0.1385). This predicts a higher value of the bulk  $c$  and hence increases the size effects. (ii) The comparison has been made between the 1-D calculation of McGurn et al. [8] and the 3-D calculation of the present analysis. The lattice structure is



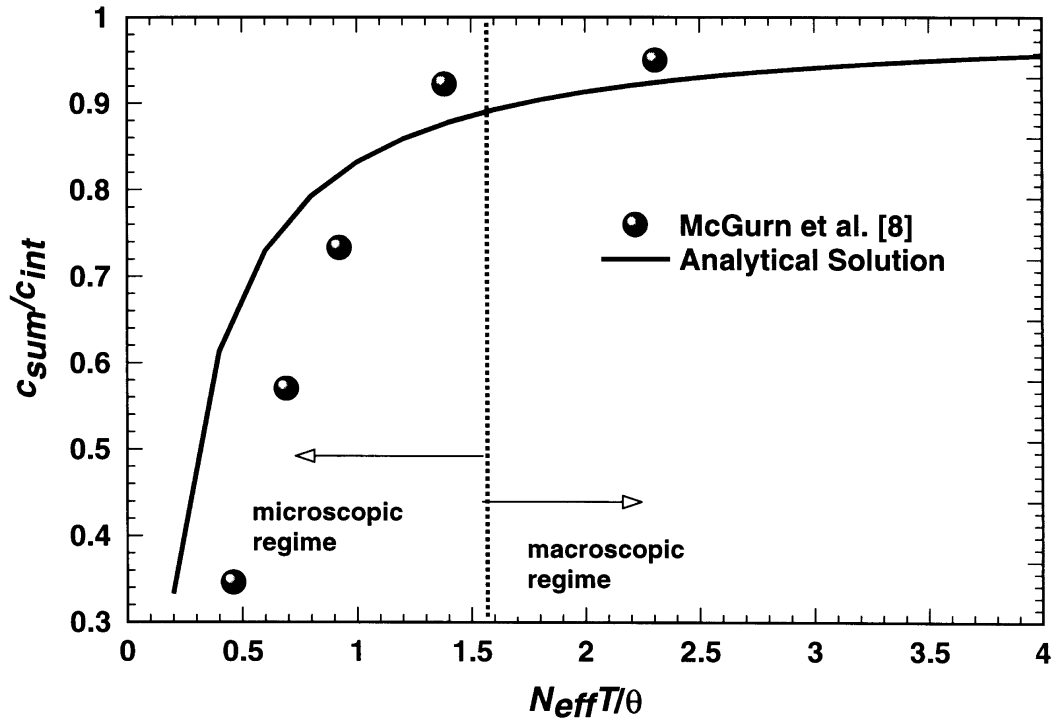


Fig. 5. Comparison between the present 3-D results and those for a 1-D linear chain of atoms presented by McGurn et al. [8].

the same for 1-D chains but can taken many different configurations for 3-D structures. This also contributes towards the discrepancy between the results of the two calculations. (iii) Finally,  $\theta$  is also a function of the interatomic potential, and for the 1-D chain it is calculated for a Lennard–Jones potential, but for the 3-D diamond lattice, the interatomic potential is not known, thus also contributing to the difference in the size effects.

### 3.1. Other thermodynamic properties

Though the calculation has been carried out for the heat capacity, the analysis can be easily extended to other thermodynamic properties utilizing the following relations [12] and assuming the solid to be completely incompressible.

$$u = \int c \, dT \quad (u \text{ is internal energy per unit volume}) \quad (40a)$$

$$s = \frac{u}{T} \quad (s \text{ is entropy per unit volume}) \quad (40b)$$

$$f = u - Ts \quad (f \text{ is Helmholtz energy per unit volume}) \quad (40c)$$

$$h = u + pV \quad (h \text{ is enthalpy per unit volume, } p \text{ is pressure and } V \text{ is volume}) \quad (40d)$$

$$g = h - Ts \quad (g \text{ is the Gibbs energy per unit volume}). \quad (40e)$$

All the above relations are evaluated at constant volume. These relations show that every thermodynamic property described above is related to the heat capacity. So, it is quite reasonable to say that every thermodynamic property described above will exhibit the same kind of size effects as  $c$  does. This is also confirmed from the result for  $u$  and  $c$  obtained in the earlier work of Prasher and Phelan [5]. Therefore, the size effect on any thermodynamic property  $H$  can be represented as:

$$\frac{H_{\text{microscopic}}}{H_{\text{bulk}}} = \Psi(R) \quad (41)$$

where  $R = N_{eff}T/\theta$  and  $\Psi(R)$  is a function of  $R$ .  $\Psi(R)$  is the same as the analytical form presented in Table 1 for heat capacity.

## 4. Discussion

A characteristic length scale analogous to the characteristic length scale for thermal conduction can also be associated with thermodynamic properties. The characteristic length scale for heat conduction is given by [13]

$$(i) \quad \frac{L}{\Lambda} < O(1) \quad \text{and} \quad \frac{L}{\lambda_c} > O(1) \quad (\text{classical size effects}) \quad (42)$$

$$(ii) \quad \frac{L}{\lambda_c} < O(1) \quad (\text{quantum effects}) \quad (43)$$

where  $\Lambda$  is the mean free path of phonons and  $\lambda_c$  the dominant phonon wavelength. For thermodynamic properties there are no classical size effects because these properties depend only on the number of excited phonons, not on the scattering of phonons. Therefore, for thermodynamic properties size effects are expected for

$$\frac{L}{\lambda_c} < O(1)$$

where  $\lambda_c$  is given by [14]

$$\lambda_c = \frac{2\pi\hbar v}{k_b T} = \frac{2\pi\theta}{k_a T} = \frac{2\pi\theta}{(6\pi^2 n)^{1/3} T} = \frac{1.611 \theta a}{(\Pi)^{1/3} T} \quad (44)$$

where  $\Pi$  is the number of atoms per unit cell. The factor  $1.611/\Pi^{1/3}$  is very close to 1 and therefore

$$\lambda_c \approx \frac{\theta a}{T} \quad (45)$$

showing that

$$\frac{L}{\lambda_c} \approx \frac{NT}{\theta} < O(1) \quad (46)$$

characterizes the onset of the microscopic region for thermodynamic properties. For 1-D structures  $NT/\theta < 1$  is suggested by Prasher and Phelan [5, 6] for prominent size effects on the thermodynamic properties. For 2- and 3-D structures  $NT/\theta < O(1)$  is more suitable. A more precise value can be determined from Fig. 4, which shows that the microscopic regime increases with the dimensionality of the structure.

There are some key issues, such as the uncertainty principle and the use of the periodic boundary condition, which need to be addressed because of the extremely small dimensions of the structures considered here. If it is assumed that the periodic boundary condition holds at such minute dimensions, although it is debatable [5, 13], then the maximum possible uncertainty in the momentum ( $\Delta p$ ) of phonons for a 1-D structure is  $\hbar\Delta k_x$ , where  $\Delta k_x$  is given by equation (2). This is because, as already discussed, the maximum contribution to the thermodynamic properties in the cryogenic regime comes from  $k_x = \Delta k_x$  and thus,  $k_x = \Delta k_x$  is the dominant wave vector. This is true even for bulk samples. The maximum uncertainty in the location of the phonons along the  $x$ -direction ( $\Delta x$ ) is  $L_x$ . The uncertainty relation is given by [15]

$$\Delta x \Delta p \geq \hbar \quad (47)$$

which upon substitution of the values of  $\Delta p$  and  $\Delta x$  reduces to

$$L_x \Delta k_x \geq 1. \quad (48)$$

Substituting  $2\pi/L_x$  for  $\Delta k_x$ , the left side of equation (48) is always equal to  $2\pi$ , be it for the bulk case or for the thin-film case, where the periodic boundary condition is applied. Therefore, within the assumptions of the periodic boundary condition, the uncertainty in the location or the momentum of the phonon is the same for a thin-film structure and a bulk solid. It can be easily shown that this holds well for 2- and 3-D structures.

The use of the periodic boundary condition is a little suspect at very small dimensions, as it is strictly valid for dimensions tending to infinity [16], but the periodic boundary condition has still been used at these minute levels for the calculation of properties, such as electronic properties [16, 17]. The heat transfer community has employed the periodic boundary condition primarily for the calculation of transport properties [18, 19].

The finite dimensions of the solid can give rise to some other interesting phenomena. The surface modes can contribute substantially to the energy of the system. In a bulk solid the contribution from the surface phonon modes is negligible. Although there have been quite a good number of experimental and theoretical studies on the contribution of the surface modes on the heat capacity of small particles [20–22], the size effect on the heat capacity due to bulk phonon modes has been neglected. Most of the work on the heat capacity of small particles has been done for approximately spherical particles having dimensions of the order of 20 Å [22], where the contribution of the surface modes becomes very prominent as the surface-to-volume ratio is very large. But the 1- and 2-D structures are semi-infinite [6] in one and two directions, respectively and it is reasonable to expect that the heat-holding capacity of the structure is primarily due to the excitation of the bulk phonon modes. Even for the 3-D structures the surface modes contribute only at extremely small dimensions [22].

It is also reasonable to expect that the Bose–Einstein statistical function will not hold for very small samples, however, Tien and Chen [13] report that it is still possible to have enough phonons to satisfy the statistics requirements.

## 5. Conclusion

This analysis indicates the presence of prominent size effects on the thermodynamic properties of microstructures due to a reduction in the filled phonon states. The Debye model can be safely assumed for predicting the size effects. A non-dimensional parameter that combines the effects of the dimensionality, temperature and the material properties (in the form of the Debye temperature), is suggested which accurately describes how the size effects vary with each of these parameters.

### Acknowledgements

The authors are deeply indebted to Sashishekara S. Talya for help in evaluating the integrals. P.E.P. gratefully acknowledges the support of the National Science Foundation through a CAREER Award (Grant No. CTS-9696003).

### References

- [1] M. Notomi, S. Nojima, M. Okamoto, H. Iwamura, T. Tamamura, Size dependence of lateral quantum-confinement effects of the optical response in  $\text{In}_{0.53}\text{Ga}_{0.47}\text{As}/\text{InP}$  quantum wires, *Physical Review B* 52 (1995) 11 073–11 088.
- [2] G. Chen, Non-local and non-equilibrium heat conduction in the vicinity of nanoparticles, *Journal of Heat Transfer* 118 (1996) 539–545.
- [3] A.B. Duncan, G. P. Peterson, Review of microscale heat transfer, *Applied Mechanics Reviews* 47 (1994) 397–428.
- [4] S.R. Mirmira, E.E. Marotta, L.S. Fletcher, Review of the thermal conductivity of thin films, *J. of Thermophysics and Heat Transfer* 12 (1998) 121–131.
- [5] R.S. Prasher, P.E. Phelan, Size effects on the thermodynamic properties of thin films, *AIAA/ASME Joint Thermophysics and Heat Transfer Conference*, Albuquerque, New Mexico, HTD-Vol. 357(3) (1998) 195–203.
- [6] R.S. Prasher, P.E. Phelan, Size effects on the thermodynamic properties of thin solid films, *J. of Heat Transfer*, to appear.
- [7] H. Grille, K. Karch, F. Bechstedt, Thermal properties of  $(\text{GaAs})\text{N}(\text{Ga}_{1-x}\text{Al}_x\text{As})\text{N}(001)$  superlattices, *Physica B* 219 and 220 (1996) 690–692.
- [8] A.R. McGurn, P. Rayan, A.A. Maradudin, R.F. Wallis, Quantum Monte Carlo calculation of the thermodynamic functions of a Lennard–Jones chain of atoms, *Physical Review B* 40 (1989) 2407–2413.
- [9] C. Kittel, *Introduction to Solid State Physics*, 6th ed., Wiley, New York, 1986, pp. 81–124.
- [10] N.W. Ashcroft, N.D. Mermin, *Solid State Physics*, W.B. Saunders, Philadelphia, PA, 1976, pp. 415–450.
- [11] J.M. Ziman, *Electrons and Phonons*, Oxford University Press, Oxford, 1996, pp. 1–61.
- [12] K. Wark, *Advanced Thermodynamics for Engineers*, McGraw-Hill, Singapore, 1998, pp. 189–195.
- [13] C.L. Tien, G. Chen, Challenges in microscale conductive and radiative heat transfer, *J. of Heat Transfer* 116 (1994) 799–807.
- [14] A. Majumdar, Microscale energy transport in solids, in: C.L. Tien, A. Majumdar, F.M. Gerner (Eds.), *Microscale Energy Transport*, Chap. 1, Taylor and Francis, Washington, DC, 1998.
- [15] P.A. Tipler, *Physics*, Worth Publishers, New York, 1980, pp. 968–969.
- [16] J. Davis, *The Physics of Low-Dimensional Semiconductors*, Cambridge University Press, New York, 1998, pp. 1–146.
- [17] Y. Arakawa, H. Sakaki, Multidimensional quantum well laser and temperature dependence of its threshold current, *Applied Physics Letters* 40 (1982) 939–941.
- [18] G. Chen, Phonon wave effects on heat conduction in thin films, *AIAA/ASME Joint Thermophysics and Heat Transfer Conference*, Albuquerque, New Mexico, HTD-Vol. 357(3) (1998) 205–213.
- [19] A. Majumdar, Microscale heat conduction in dielectric thin films, *J. of Heat Transfer* 115 (1993) 7–16.
- [20] G.D. Zally, J.M. Mochel, Fluctuation contribution to the heat capacity of amorphous superconducting films, *Physical Review B* 6 (1972) 4142–4150.
- [21] R.F. Allen, F.W. De Wette, Calculation of dynamical surface properties of noble-gas crystals, *Physical Review* 179 (1969) 873–886.
- [22] V. Novotny, P.P.M. Meincke, Thermodynamic lattice and electronic properties of small particles, *Physical Review B* 8 (1973) 4186–4199.